International Journal of Engineering Research & Technology (IJERT)
ISSN: 2278-0181
Vol. 9 Issue 07, July-2020

Seismic Behavior of HSC Eccentric Beam-Column Connections

Mahmoud A. El-Mandouh*
* Civil Construction Department, Beni-Suef University,
Beni-Suef 62521, Egypt

***Abstract*:- Analytically studied of six full-scale High-strength reinforced concrete (HSC with f_c' = 75 MPa) and Normal-strength reinforced concrete (NSC with f_c' = 25 MPa) eccentric beam-column connections under seismic loading have been carried using the finite element computer software ANSYS. The applicability of the joint shear force provisions used by international codes; e.g., the American Concrete Institute (ACI 318-14), the New Zealand Code (NZS-2006) and the Eurocode 2 (EC-2) are examined when applied to HSC eccentric beam-column connections. The main investigated parameters are concrete strength and a beam's eccentricity relative to the column. The ultimate failure load of connection with beam side at the column edge is less than that of the reference connection (without beam eccentricity) by about 55% for connections constructed from NSC, while the ultimate failure load reduced by about 25% for the same connections constructed from HSC. The calculated joint shear force using the ACI 318-14 equations is conservative for NSC and more conservative for HSC eccentric beam-column connections. The joint shear force predicted using the equations of NZS-2006 is more conservative for both NSC and HSC eccentric beam-column connections; on the opposite, the situation is reversed for HSC when the EC-2 is applied. Though the ACI 318-14 limits the eccentricity between the beam and the column centerlines to 1/8 of column width, it has been found that the eccentricity of 15% of the column width is still on the safe side as predicted the ACI 318-14 for HSC connections.**

Keywords: Reinforced concrete; seismic response; nonlinear analysis; failure; joint shear strength

1. INTRODUCTION

In most cases of construction beam-column connections it is often required to construct eccentric beam relative to column, this eccentricity between the beam and column contributes to the creation of torsion in the contact region parallel to the exterior edge of the structure under lateral loading. This torsion in the joint creates extra shear stress and can adversely affect the joint's inelastic behavior. Most studies are devoted to the seismic behavior of reinforced concrete beam-column joints, constructed from NSC with compressive strength less than 40 MPa. With widespread use of HSC with compressive strength approaching 140 MPa [1], studying the seismic behavior of the HSC eccentric beam-column connections has become necessary. Present design guidelines [2] are focused on limited experimental work on eccentric connections and take into account post-earthquake observations [5] of increased damage to external connections between the beam and the column centerlines. Previous [27] indicated that beam eccentricity leads to unsymmetric damage in the joint due to additional shear stresses caused by torsion. This damage resulted in pinched load-versus drift hysteresis curves for the subassemblies and low energy dissipation capacities. Consequently, in the recommendations of the ACI Committee 352, the shear strength of the eccentric beam-column connections is decreased by using a smaller effective joint width if the eccentricity of the beam to column centroide exceeds 1/8 of the column width.

The investigation's main objective is to research the seismic behavior of both NSC and HSC eccentric exterior beam-column connections and draw an analogy between both types of connections. The finite element method is utilized via the software ANSYS to expand this analysis. The applicability of the provisions on joint shear force used by international codes; e.g., the American Concrete Institute [4], the New Zealand Code [22] and the Eurocode 2 [11] are investigated when applying to HSC eccentric beam-column connections.

2. CODES PROVISIONS

2.1 ACI 318 -14

The joint shear design force across a connection V_{jh} shall be taken as follows:

$V_{jh} = 1.70\sqrt{f_c'}A_j$ for connections confined to all four faces by beams (1)

$V_{jh} = 1.20\sqrt{f_c'}A_j$ for connections confined to three faces by beams (2)

$V_{jh} = 1.0\sqrt{f_c'}A_j$ for other cases (3)

$A_j = b_j * h_c$ (4)

International Journal of Engineering Research & Technology (IJERT)
ISSN: 2278-0181
Vol. 9 Issue 07, July-2020

$$b_j = the\ smallest\ of\ (b_b + 2x)\ or\ (b_b + h_c) \quad (5)$$

where f_c' is the cylinder compressive strength of the concrete, A_j is the effective cross-sectional area within a connection, b_j is the effective joint width, b_b is the beam width, h_c is the column depth and x is the smaller distance from beam edge to column side.

2.2 NZS-2007

The joint shear design force across a connection V_{jh} is the least of the subsequent values:

$$V_{jh} = 0.20 f_c' b_j h_c \quad (6.a)$$

$$V_{jh} = 10 b_j h_c \quad (6.b)$$

where h_c is the same as for the ACI 318 -14 and b_j is the effective joint width and shall be taken the smaller of beam width, b_b or $(b_c + 0.50h_c)$. Where b_c is the column width. For eccentric beam-column connection, b_j shall not exceed $0.50(b_b + b_c + 0.50h_c) - e$, where e is the beam's eccentricity relative to column.

2.3 EC-2

The joint shear design force across a connection V_{jh} shall be taken as:

$$V_{jh} < 0.50 \alpha_c \upsilon f_{cd} b_j h_c \quad (7)$$

$$\upsilon = 0.60\left(1 - \frac{f_{ck}}{250}\right) \quad (8)$$

where f_{ck} and f_{cd} is the characteristic and the design value of concrete compressive strength, respectively. The factor α_c in the Eq. (7) shows the effects of confining pressure (n_{jy}) on the compressive strength of the diagonal strut:

$$\alpha_c = 1 + 2(n_{jy} + \rho_y f_{sd})/f_{cd} \le 1.50 \quad (9)$$

where $\rho_y = A_{sy}/(h_b h_c)$ is the reinforcement ratio of stirrups in the transverse direction y, and $f_{sd} = 300MPa$ is a reduced stress of this transverse reinforcement, for limitation of cracking. The horizontal design sheer force of exterior joints is taken as 80% of the value given by Eq. (7). The effective joint width b_j is the same as for the NZS-2007.

2. ANALYSIS PROGRAM

The six of full-scale beam-column connections as illustrated in Fig- 1 were studied. The beam length and column height is bounded by the lines of contraflexure. All the beams have the same cross section 200x 400 mm. The column cross section is (450*450 mm) and its total height is 2000mm [14]. The strong column-weak beam philosophy was used in the design of all connections to ensure the production of beam plastic hinging at large displacements, rather than column-plastic hinging. The beams of all connections were reinforced equally top and bottom with three longitudinal bars of 16mm diameter for one bar. The columns of all connections were reinforced with longitudinal 4 bars with diameter 16mm for one bar. The stirrups of diameter 10 mm every 100 mm were used for both column and beam of all connections. The yield stress for beam and column reinforcement of the longitudinal bars and transverse bars was 360 MPa and 280MPa, respectively.

The principal parameters of the analysis are the beam's eccentricity relative to the column and concrete strength. The six connections included three connections with (Normal strength concrete with f_c' = 25 MPa) and three connections with (High strength concrete with f_c' = 75 MPa). Three different beam positions were studied; the first beam location is the beam axis identical to the column axis, the second beam position the eccentricity of the centerlines between the beam and column equal to 60mm (i.e. 15% of column depth), and the third beam position the beam side at the column edge. Fig- 2(a) and Fig- 2(b) show the studied connections designation, and the beam location in the NSC and HSC connections, respectively.

International Journal of Engineering Research & Technology (IJERT)
ISSN: 2278-0181
Vol. 9 Issue 07, July-2020

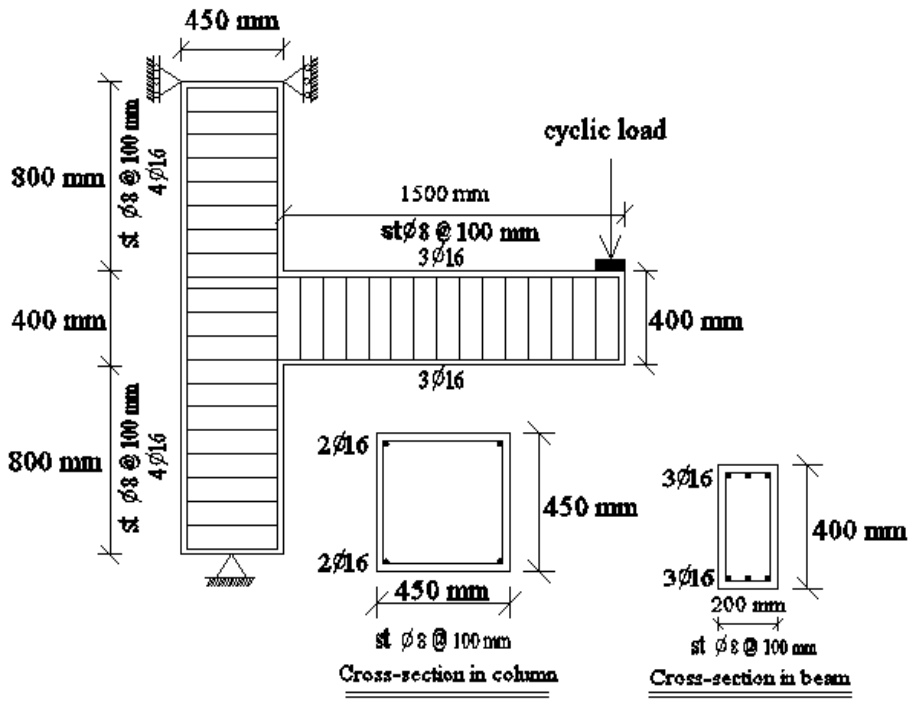

Fig- 1: Dimensions and Boundary Conditions of Study Connections

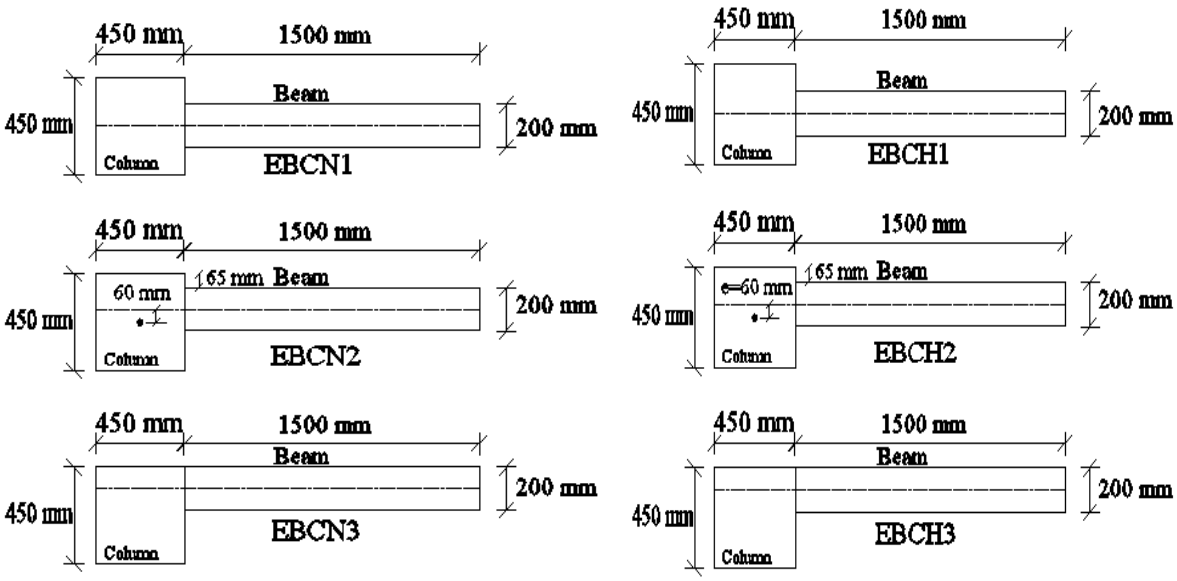

(a) NSC (b) HSC

Fig- 2: Plan view of studied beam-column connection

4. FINITE ELEMENT ANALYSIS

4.1 Validation of the Model

With the comparison of the experimental program [14] and analytical results, the validation of the current model it has achieved of the range of 91-93% as shown in Fig- 3, this disparity in results due to the effect of the boundaries conditions and assuming of the full bond between reinforcement and concrete.

International Journal of Engineering Research & Technology (IJERT)
ISSN: 2278-0181
Vol. 9 Issue 07, July-2020

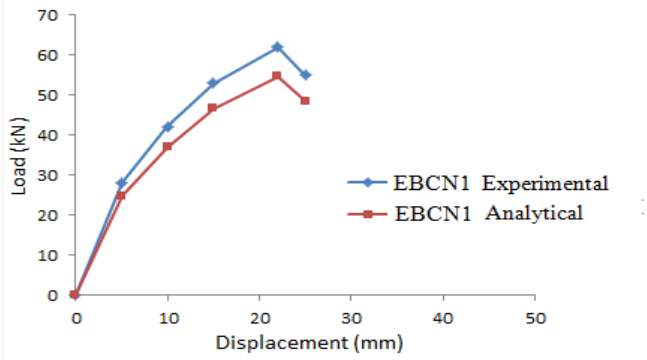

Fig- 3: Comparison between the experimental and analytical results of beam-column EBCN1

4.2 Finite Element Modeling

3D nonlinear Finite Element Analysis using the software ANSYS [3] has been performed to study the performance of eccentric beam-column connections with (Normal strength concrete with f_c' = 25 MPa and High strength concrete with f_c' = 75 MPa). The concrete was modeled with solid element SOLID65; this element has eight nodes and has three degrees of freedom for each node, nodal translations in x, y, and z directions. The bars were modeled with a series of two-node link elements LINK 180; at each node this element has three degrees of freedom.

4.3 Reinforcement

The one bar area of longitudinal beam and column reinforcement is 201.00 mm2. The modulus of elasticity, E_S , was defined as 2*10^5 MPa and the Poisson's ratio was taken equal to 0.30. The yield strength of longitudinal and transverse reinforcement was equal to 360 MPa and 280 MPa, sequentially. A Perfect bond was expected between rebar and concrete.

4.4 Concrete

The elasticity modulus of concrete was calculated according to the ACI 318-14 formula which gave values of 23500.0 MPa and 35652.04 MPa, for concrete with f_c' equal to 25 MPa, and 75 MPa, sequentially.

$$E_c = 4700\sqrt{f_c'} \quad \text{for NSC} \tag{10}$$

$$E_c = 3320\sqrt{f_c'} + 6900 \quad \text{for HSC} \tag{11}$$

The concrete Poisson's ratio was assumed to equal to 0.2. The following equation shows the uniaxial compressive stress–strain values of concrete [9]:

$$f = E_c \varepsilon / ((1 + (\varepsilon / \varepsilon_0)^2) \tag{12}$$

$$\varepsilon_0 = 2f_c' / E_c \tag{13}$$

where ε is the strain at the compressive stress f in MPa and ε_0 is the strain at the maximum stress, f_c'.

The uniaxial tensile cracking stress according to ACI 318-14, f_t , is

$$f_t = 0.62\sqrt{f_c'} \tag{14}$$

4.5 The Finite Element Mesh

In order to obtained accurate results all elements have the same mesh size. The type of mesh selected in the model is Hex/wedge. The concrete solid element SOLID65 is the mesh element for concrete and its size 50 mm* 50 mm* 50 mm. The link element LINK 180 is the mesh element for rebar with mesh 50mm. Fig. 4 shows concrete volume meshes for reference exterior beam-column connection.

4.6 Boundary Condition and Load History

Loading and boundary conditions were performed in the model of exterior beam-column connections to simulate the

International Journal of Engineering Research & Technology (IJERT)
ISSN: 2278-0181
Vol. 9 Issue 07, July-2020

experimental test setup [14] as shown in Fig- 4. The base of the lower column was hinged $u_1 = u_2 = u_3 = 0.0$ and the top of the upper column was roller $u_1 = u_3 = 0.0$. The right edge of the beam was loaded by reversed loading as shown in Fig- 5 to simulate the beam-column connections under earthquake loading.

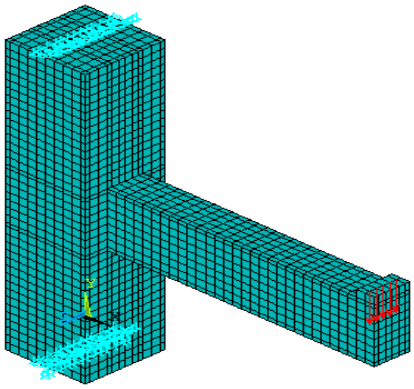

Fig- 4: Concrete volume meshes for exterior beam-column connection EBCN1

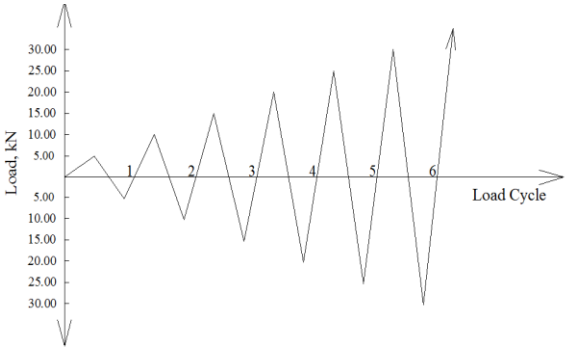

Fig- 5: Load sequence diagram

5. ANALYSIS of RESULTS

5.1 Crack Pattern

All beams failed with the crack patterns shown in Fig- 6(a) to Fig- 6(f). As presented in Table- 1, the initial crack of reference connection EBCN1(the centerlines of the beam and column are coincide) was observed at a load of approximately 40% of the failure load, most cracks seemed first at a distance 50mm from the column face also extend to the beam edge. For connections EBCN2 (eccentricity equal to 60mm between the centerlines of the beam and column, i.e. 15% of column depth) and EBCN3 (the beam side at the column edge), the initial crack was observed at a load value of approximately 55% and 53%, respectively. Most cracks appeared for connections EBCN2 and EBCN3 first at the column face and not extend to the column edge.

The crack pattern of all studied HSC exterior beam-column connections was analogous to this of NSC connections. For connections EBCH1, EBCH2 and EBCH3, the initial crack was observed at a load of approximately 39-45% of the failure load. Though the ACI 318-14 limits the eccentricity between the beam and the column centerlines to 1/8 of column width, it has been found that the eccentricity of 15% of the column width is still on the safe side as predicted the ACI 318-14 for HSC connections. These results indicate that, the cracks were initiated in the exterior beam-column connections from NSC at loads lower than those of that from HSC; 50-75%.

Table- 1: Summary of analysis results

Exterior beam-column connection	Ultimate failure load (kN)	Ultimate vertical beam displacement just before failure (mm)	First crack load (kN)
EBCN1	50.29	23.25	20.30
EBCN2	23.10	8.40	12.90
EBCN3	22.44	7.95	11.90
EBCH1	64.83	46.73	26.90
EBCH2	61.30	29.85	24.40
EBCH3	48.53	13.82	22.30

International Journal of Engineering Research & Technology (IJERT)
ISSN: 2278-0181
Vol. 9 Issue 07, July-2020

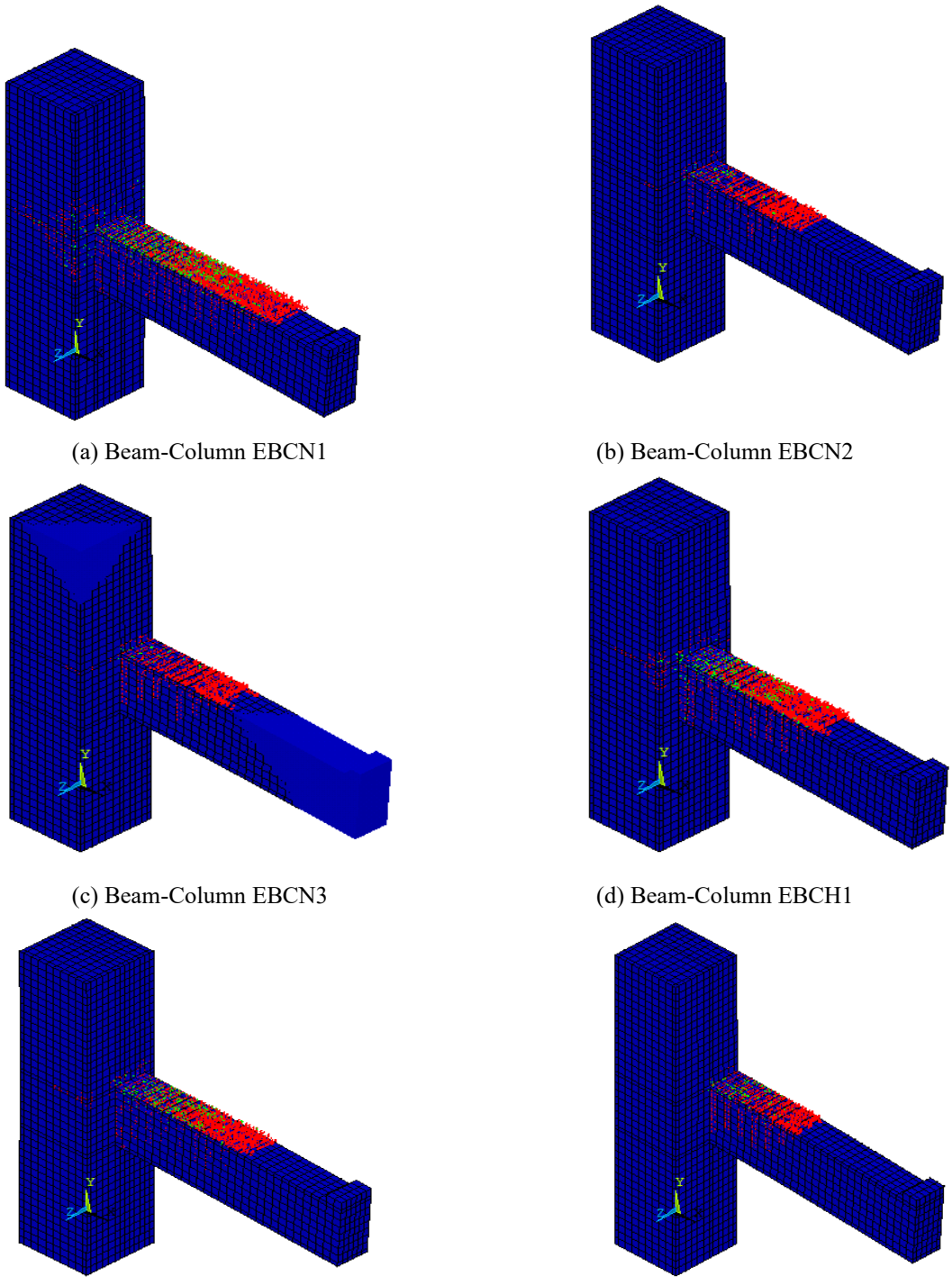

(a) Beam-Column EBCN1 (b) Beam-Column EBCN2

(c) Beam-Column EBCN3 (d) Beam-Column EBCH1

(e) Connection EBCH2 (f) Connection EBCH3

Fig- 6: Crack pattern of studied beam-column connections

5.2 Ultimate Strength

The ultimate failure load is affected by concrete strength and beam eccentricity as observed from the results in Table 1, the maximum equivalent Von-Misses for all studied beam-column connections as shown in Fig- 7(a) to Fig- 7(f). For NSC connections, the ultimate failure load of connections EBCN2 and EBCN3 is smaller than that of the connection EBCN1 (the centerlines of the beam and column are coincide) by approximately 54% and 55%, sequentially. For HSC connections, the ultimate failure load of connections EBCH2 and EBCH3 is smaller than that of the connection EBCH1 (the centerlines of the beam and column are coincide) by approximately 5% and 25%, sequentially. It became clear that use high strength concrete

International Journal of Engineering Research & Technology (IJERT)
ISSN: 2278-0181
Vol. 9 Issue 07, July-2020

greatly enhanced the overall performance of the eccentric connection and delayed degradation of joint shear stiffness and strength. These results indicate that, increasing the concrete strength from NSC (with f_c' = 25 MPa) to HSC (with f_c' = 75 MPa**)** led to a clear rise in the ultimate failure load of the connections with the centerlines of the beam and column are coincide by approximately 29%; by 165% for connections that the distance between the centerlines of the beam and column equal to 60mm , i.e. 15% of column depth; by 116% for connections with the beam side at the column edge. Also the results indicate that, when using NSC, the effect of the distance between centerlines of the beam and column on the ultimate failure load is clear on the opposite side when using HSC. Also, though the ACI 318-14 limits the eccentricity between the beam and the column centerlines to 1/8 of column width, it has been found that the eccentricity of 15% of the column width is still on the safe side as predicted the ACI 318-14 for HSC connections.

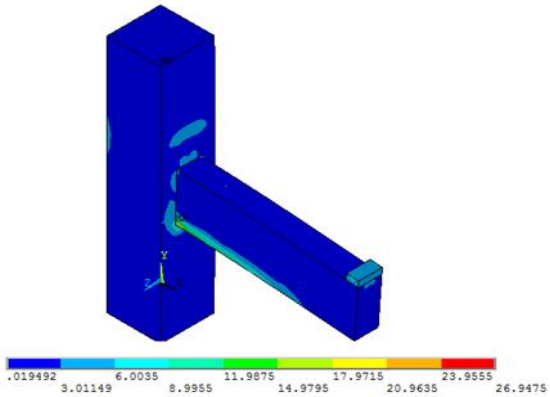

(a) Beam-Column EBCN1

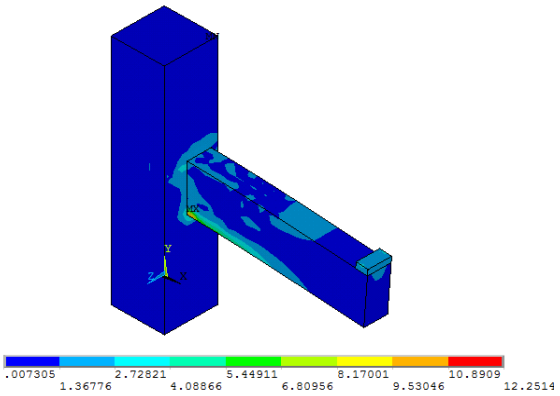

(b) Beam-Column EBCN2

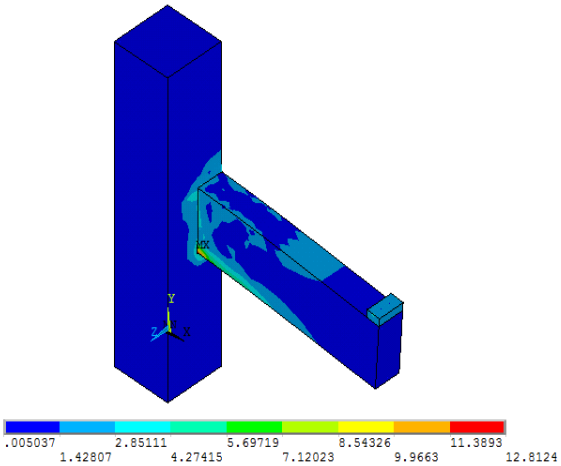

(c) Beam-Column EBCN3

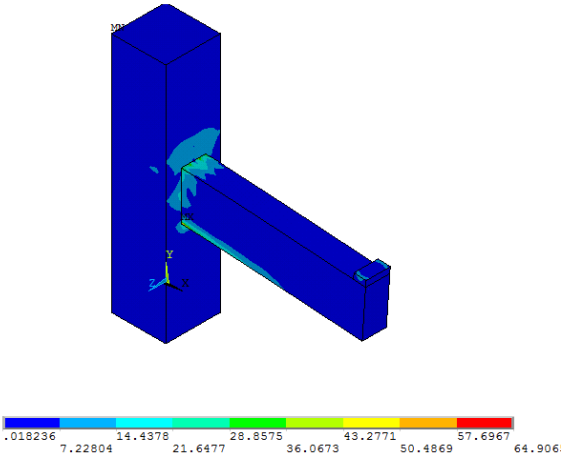

(d) Beam-Column EBCH1

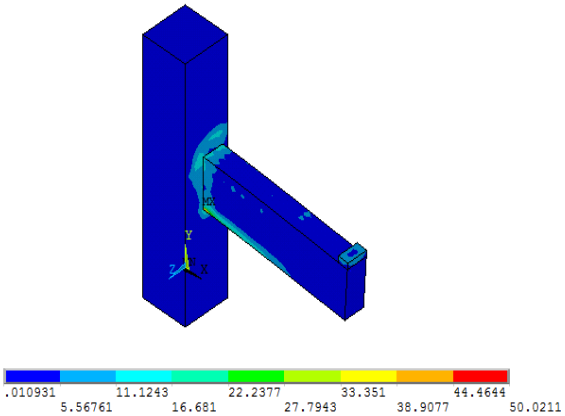

(e) Beam-Column EBCH2

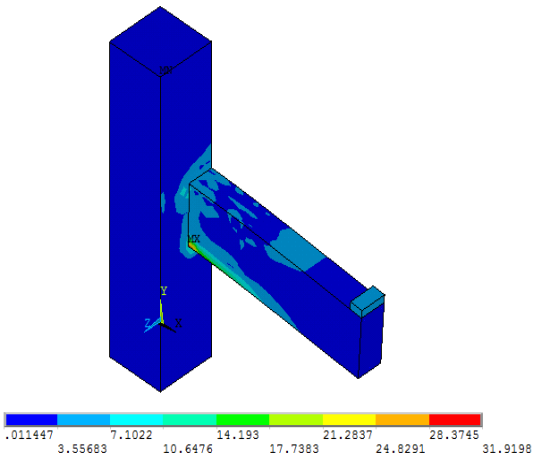

(f) Beam-Column EBCH3

Fig- 7: Maximum equivalent Von-Misses of studied beam-column connections

International Journal of Engineering Research & Technology (IJERT)
ISSN: 2278-0181
Vol. 9 Issue 07, July-2020

5.3 Reinforcement Strains

Fig- 8(a) to Fig- 8(f) indicate the rebar strains in the beam's upper and lower longitudinal reinforcement. It has been noted, for NSC beam-column connections the strains in the longitudinal beam reinforcement don't reach to yielding, on the other hand, the situation is reversed for HSC beam-column connections. For HSC connections, the load producing first steel yield in connections EBCH2 and EBCH3 is smaller than that of the reference connection EBCN1 by approximately 8% and 27%, sequentially. In the case of NSC connections, the initial crack load is lower than that of similar HSC connections; around 50-75%. Also, it has been noticed that, the strain distributions for all HSC beam-column connections are similar.

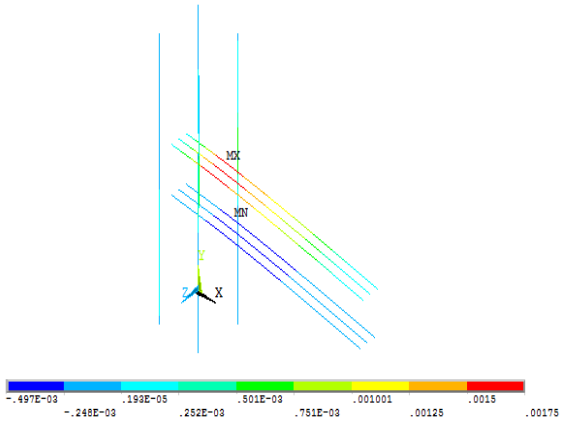

(a) Beam-Column EBCN1

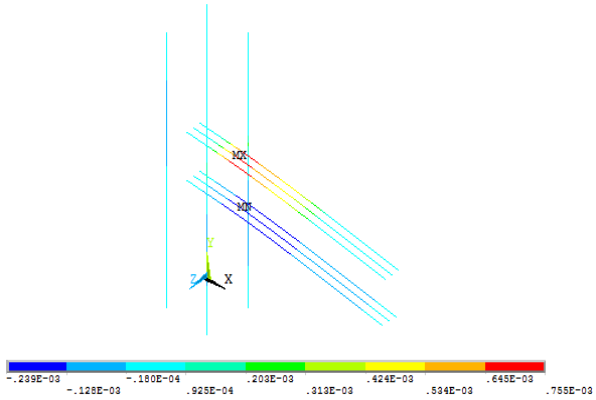

(b) Beam-Column EBCN2

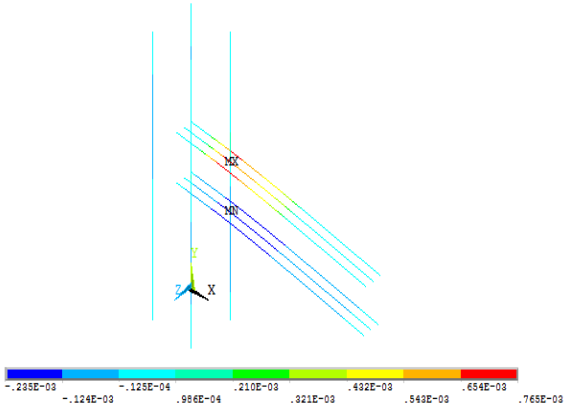

(c) Beam-Column EBCN3

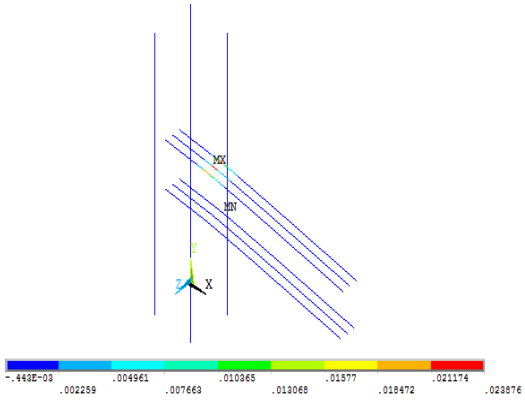

(d) Beam-Column EBCH1

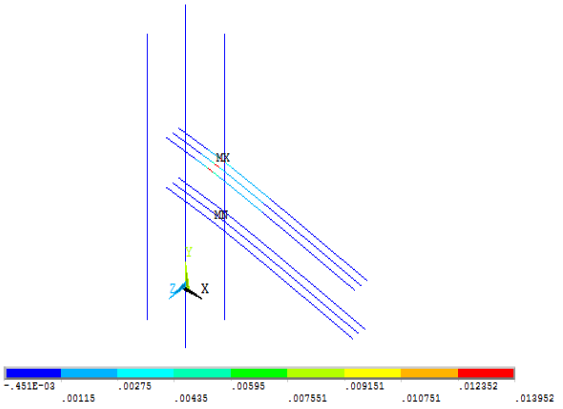

(e) Beam-Column EBCH2

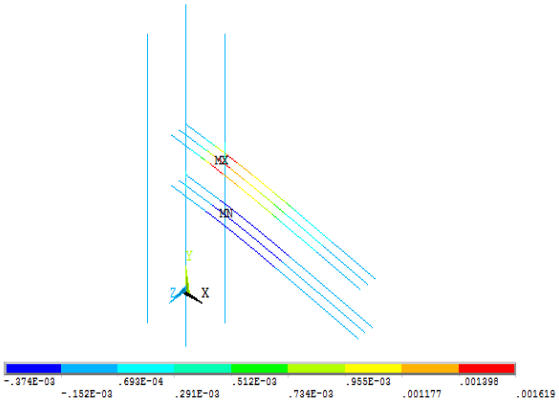

(f) Beam-Column EBCH2

Fig- 8: Reinforcing bar strain of studied beam-column connections

International Journal of Engineering Research & Technology (IJERT)
ISSN: 2278-0181
Vol. 9 Issue 07, July-2020

5.4 Hysteretic Lateral Vertical Loading Curves versus Beam Edge Displacement

Fig- 9(a) to Fig- 9(f) show the hysteretic lateral vertical loading curves versus edge beam displacement for all the studied connections. Table-1 gives the lateral load peak values immediately before failure with the vertical displacement at the beam edge. The maximum displacement at the beam edge for connections EBCN2 and EBCN3 is smaller than that of the reference connection EBCN1 by approximately 64% and 65%, sequentially. Whereas, the maximum vertical displacement at the beam edge for EBCH2 and EBCH3 is smaller than that of the corresponding reference connection EBCH1 by approximately 36% and 70%, sequentially. From the above results, the maximum vertical displacement at the beam edge of the HSC connections is larger than that of the connections from NSC by about 73-95%.

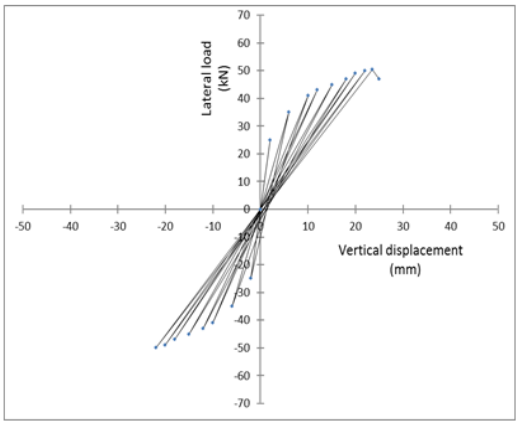

(a) Beam-Column EBCN1

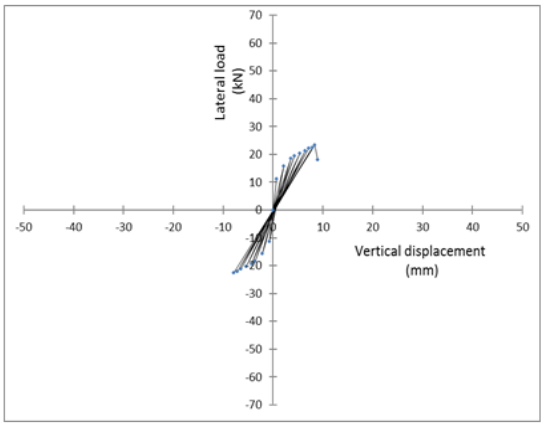

(b) Beam-Column EBCN2

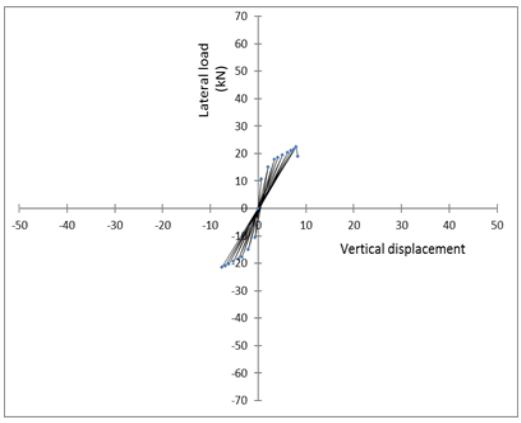

(c) Beam-Column EBCN3

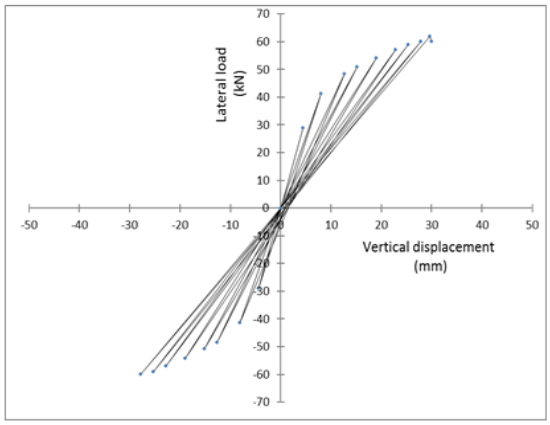

(d) Beam-Column EBCH1

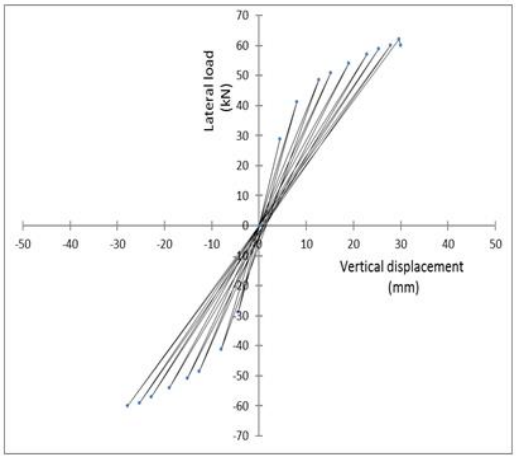

(e) Beam-Column EBCH2

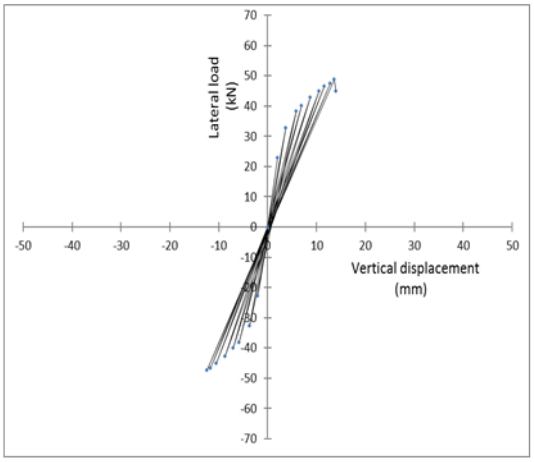

(f) Beam-Column EBCH3

Fig- 9: Hysteretic loop for studied beam-column connection

International Journal of Engineering Research & Technology (IJERT)
ISSN: 2278-0181
Vol. 9 Issue 07, July-2020

6. COMPARISON of RESULTS with CODES PROVISIONS

The envelops of the analytical joint shear forces of the studied connections are compared with that calculated from studied international codes as shown in Table- 2. This contrast illustrates the joint shear force estimated utilizing the ACI 318-14 equations is conservative for NSC and more conservative for HSC eccentric beam-column connections. The joint shear predicted using the equations of NZS-2006 is more conservative for both NSC and HSC eccentric beam-column connections; by contrast, the situation is reversed for HSC when the EC-2 is applied.

Table- 2: Comparison between the analytical joint shear force and that predicted using the equations of the studied international codes

Beam-column connection	Analytical joint shear force (kN)	Joint shear force according to the studied international codes (kN)		
		ACI 318-14	NZS-2006	EC-2
EBCN1	1113.75	1012.50	450.00	911.25
EBCN2	746.80	742.50	450.00	911.25
EBCN3	451.00	450.00	450.00	911.25
EBCH1	3654.50	1753.70	900.00	3543.70
EBCH2	2652.75	1286.05	900.00	3543.70
EBCH3	1593.67	779.42	900.00	3543.70

5. CONCLUSIONS

The following can be understood from the findings of this analytical investigation:

1- For NSC connections, the ultimate failure load of connection that the distance between the centerlines of the beam and column equal to 15% of column depth is less than that of the reference connection by about 54%, while the ultimate failure load reduced by about 5% for the same HSC connections.

2- For NSC connections, the ultimate failure load of connection for beam side at the column edge is less than that of the reference connection by about 55%, while the ultimate failure load reduced by about 25% for the same HSC connections.

3- The joint shear force estimated utilizing the ACI 318-14 equations is conservative for NSC and more conservative for HSC eccentric beam-column connections.

4- The joint shear predicted using the equations of NZS-2006 is more conservative for both NSC and HSC eccentric beam-column connections; by contrast, the situation is reversed for HSC when the EC-2 is applied.

5- When using NSC, the effect of the distance between centerlines of the beam and column on the ultimate failure load is clear on the opposite side when using HSC.

6- Though the ACI 318-14 limits the eccentricity between the beam and the column centerlines to 1/8 of column width, it has been found that the eccentricity of 15% of the column width is still on the safe side as predicted the ACI 318-14 for HSC connections.

REFERENCES

[1] ACI Committee 363, (1992) State-of-the-art report on higher-strength concrete. *ACI 363R-92, American concrete Institute*, Farmington, Hills, MI, 55 P.

[2] ACI-ASCE Committee 352, (1988) Recommendations for design of RC beam-column connections in monolithic reinforced concrete structures. *ACI Structural Journal*, 85(6), 675-696.

[3] ANSYS User's Manual, (2010), Teory, Commands, Analysis and Element, Release 12 ANSYS Inc. Houston, Pa.

[4] American Concrete Institute, ACI 318, (2014), Building Code Requirements for Structural Concrete, *ACI 318-14, ACI Committee 318*, 503 pp., Detroit, USA.

[5] Arai-Gumi Technical Research Institute, (1999) Special issue investigation report on the 1995 Hyogen-Nambu Earthquake. Arai Technical Research Report, Hyogo, Japan, 113 pp.

[6] Burak B., (2005) Seismic behavior of eccentric reinforced concrete beam-column-slab Connections. *Ph.D. Thesis*, *the University of Michigan*, Ann Arbor.

[7] Burak B. and Wight J.K. (2008) Experimental investigation on seismic behavior of eccentric reinforced concrete beam-column-slab connections. *ACI Structural J.*, 105(2), 154-162.

[8] Chen C.C. and Chen G., (1999) Cyclic behavior of reinforced concrete eccentric beam-column corner joints connecting spread-ended beams. *Structural J.*, 96(3), 443-449.

[9] Desayi P., and Krishnan S., (1964) Equation for the stress-strain curve of concrete. *Journal of the American Concrete Institute*, 61(3), 345 -350.

[10] Durrani A. J. and Wight J. K., (1985) Behavior of interior beam-to-column connections under earthquake-type loading. *ACI Structural J.*, 82(3), 343-349.

[11] Eurocode 2, (2004) Design of concrete structures, Part 1-6: General rules and rules for buildings. *European Prestandard*, European committee for standardization, 253 pages.

[12] Egyptian Code Committee 203, (2008) Egyptian code of practice for design and construction of reinforced concrete structures. *Housing and Building Research Centre*, Cairo.

[13] International Code Council, (2012) *International Building Code*. Country club hills, Ill, ICC.

[14] Ibrahim G., and Osama A., (2018) Experimental behavior of full-scale exterior beam-column space joints retrofitted by ferrocement layers under cyclic loading. *Case Studies in Construction Materials*, 8, 61-78, DOI:org/10.1016/j.cscm.2017.11.002.

[15] JSCE, (2008) Standard specifications for concrete structures 2007. Design.

[16] Joh, O.; Goto, Y.; and Shibata, T., (1991) Behavior of reinforced concrete beam-column joints with eccentricity, Design of beam-column joints for seismic resistance. SP-123, J. O. Jirsa, ed., American Concrete Institute, Farmington Hills, MI, pp. 317-357.

International Journal of Engineering Research & Technology (IJERT)
ISSN: 2278-0181
Vol. 9 Issue 07, July-2020

[17] Kusuhara F., Azukawa K., Shiohara H., and Otani S., (2004) Tests of reinforced concrete interior beam-column joint subassemblage with eccentric beams. *Proceedings of the 13th World Conference on Earthquake Engineering*, Paper No. 185, Vancouver, BC, pp 14.
[18] Lawrance G.M., Beattie G.J., and Jacks D.H., (1991) The cyclic load performance of an eccentric beam-column joint (Report 91-25126). *Central Laboratories*, Lower Hutt, New Zealand, 1991, pp 81.
[19] Lee H.J. and Ko J., (2007) Eccentric reinforced concrete beam-column connections subjected to cyclic loading in principal directions. *ACI Structural J.*, 105(3), 380-382.
[20] Kim J. and LaFave J., (2008) Probabilistic joint shear strength models for design of RC beam-column connections. *ACI Structural J.*, 105(6), 770-780.
[21] LaFave J.M., and Shin M., (2005) Eccentric beam-column connections-performance and design of joints subjected to seismic lateral load reversals. *Concrete Int.*, 58-62, DOI:10.1061/41031(341)166.
[22] New Zealand Standard NZS 3101 (2006): Part 1, Concrete Structures Standard, Standards New Zealand, Wellington.
[23] Shin M., and LaFave J.M., (2004) Seismic performance of reinforced concrete eccentric beam-column connections with floor slabs. *ACI Structural Journal*, 101(3), 403-412.
[24] Teng S., and Zhou H., (2003) Eccentric reinforced concrete beam-column joints subjected to cyclic loading. *ACI Structural Journal*, 100(2), 139-148.9.
[25] Vollum R.L., and Newman J.B., (1999) Towards the design of reinforced concrete eccentric beam-column joints. *Magazine of Concrete Research*, 51(6), 397-407.
[26] Burcu B. Canbolat and James K. Wight, (2008) Experimental investigation on seismic behavior of eccentric reinforced concrete beam-column-slab connections. ACI Structural Journal, V. 105(2).
[27] LaFave, J. M., and Wight, J. K., (1999) Reinforced Concrete Exterior WideBeam-Column-Slab Connections Subjected to Lateral Earthquake Loading. ACI Structural Journal, V. 96 (4), July, pp. 577-585.

BIOGRAPHIES

Civil Construction Department, Beni-Suef University,
Al-mansoura 35511, Egypt